Compositionally Modulated Ripples Induced by Sputtering of Alloy Surfaces

V. B. Shenoy,* W. L. Chan, and E. Chason

Division of Engineering, Brown University, Providence, Rhode Island 02912, USA

(Received 8 February 2007; published 20 June 2007)

Sputtering of an amorphous or crystalline material by an ion beam often results in the formation of periodic nanoscale ripple patterns on the surface. In this Letter, we show that, in the case of alloy surfaces, the differences in the sputter yields and surface diffusivities of the alloy components will also lead to spontaneous modulations in composition that can be in or out of phase with the ripple topography. The degree of this *kinetic* alloy decomposition can be altered by varying the *flux* of the ion beam. In the high-temperature and low-flux regime, the degree of decomposition scales linearly with the ion flux, but it scales inversely with the ion flux in the low-temperature, high-flux regime.

DOI: 10.1103/PhysRevLett.98.256101 PACS numbers: 81.16.Rf, 68.35.Fx, 79.20.Rf

It is well known that periodic surface patterns can be spontaneously induced by ion-beam-assisted etching of amorphous and crystalline materials. In many cases, the feature sizes of the observed ripple and dot patterns are in the nanometer scale, making them potentially suitable for sublithographic surface templating. In a classic 1988 paper, Bradley and Harper (BH) [1] showed that the formation of ripple patterns can be understood on the basis of a competition between the surface roughening caused by the ion beam and the smoothening induced by surface diffusion. While experiments in different material systems have confirmed various aspects of their analysis, more detailed theoretical refinements have also been incorporated to the original model [2]. Given the success of these models in describing pattern formation in elemental materials, a natural question to ask is if a similar description can be developed for the sputtering of alloy materials.

In this Letter, we show that sputtering of alloy surfaces can spontaneously lead to *kinetic* surface decomposition of the alloy at the peaks and the valleys of the ripples. While the relative phase between the ripple height and composition is found to depend on the ratios of the yields and diffusivities of the alloy components, the magnitude of the *ion flux* can be altered to control the degree of alloy decomposition. Sputtering can therefore be used as a tool to simultaneously achieve nanoscale patterning of both the surface topography and composition. In what follows, we derive equations for the evolution of the height and composition modulations on sputtered alloy surfaces and study the instabilities resulting from the coupling between these modulations.

Let the sputtered surface be located in the xy plane, and let θ denote the polar angle made by the incident beam as shown in Fig. 1. For an ion flux F, let Y_A and Y_B denote the sputter yields from the elemental surfaces of species A and B, respectively. Then, for an AB alloy, the fluxes of sputtered A and B atoms are taken to be $F_A = FY_Ac_s$ and $F_B = FY_B(1 - c_s)$, respectively, where c_s denotes the fraction of lattice sites at the surface occupied by A atoms—the sputter yield for a given species is then proportional to its surface composition. For *steady state* sputtering of a planar surface, however, the fluxes of eroded atoms should also be proportional to their bulk composition, or

$$\frac{F_A}{F_B} = \frac{c_b}{1 - c_b}. \tag{1}$$

If $Y_A \neq Y_B$, this condition necessarily leads to a steady state *kinetic* surface composition, which can be obtained by solving Eq. (1) as

$$c_s = \frac{Y_B c_b}{Y_A(1 - c_b) + Y_B c_b}. \tag{2}$$

This equation predicts that the surface is enriched in the A (B) species when Y_B is large (small) compared to Y_A. In our analysis, we restrict attention to the regime where bulk diffusion is negligible compared to surface diffusion (as in the BH [1] and other related models [2]) and use Δ (of the order of a few atomic spacings) to denote the thickness of the surface layer with composition c_s.

Next, we consider the time evolution of height and composition perturbations $h(x, y, t)$ and $\zeta(x, y, t)$ (refer to Fig. 1) applied to the steady state surface profile. For the

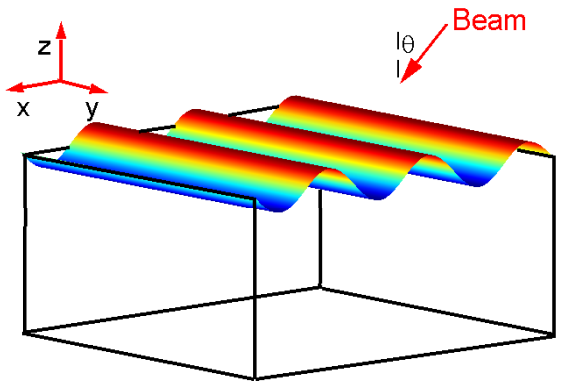

FIG. 1 (color online). Schematic of a sinusoidal surface perturbation with a wave vector along the x direction induced by an ion beam incident in the xz plane at an angle θ. The height modulations will also lead to gradients in composition, as indicated by the color variations along the surface.

perturbed surface, the change in the flux of sputtered atoms, to linear order in h and ζ, can be written as $\delta F_i = FY_i(\zeta_i - c_i\nu_h)$, where i corresponds to A or B species, $\zeta_A = -\zeta_B = \zeta$, $c_A = c_s$, $c_B = 1 - c_s$, and

$$\nu_h = \left(\nu_0(\theta)\frac{\partial h}{\partial x} + G_x(\theta)\frac{\partial^2 h}{\partial x^2} + G_y(\theta)\frac{\partial^2 h}{\partial y^2}\right) \quad (3)$$

gives the slope and curvature dependence of the sputter yield. The coefficients multiplying the derivatives of the height in ν_h are given in the work of BH [1]. Within their model, the rate of material erosion is determined by the power deposited at a given point due to the slowing down of the implanted ions. Here, for simplicity, we have assumed that the average depth of penetration of the ions and the spatial distribution of energy deposition from the beam is independent of the alloy composition. Therefore, once the yields Y_i of the individual species are given, the coefficients ν_0, G_x, and G_y in ν_h will be the same for both species of atoms. The perturbations also lead to a diffusive surface mass current, given by

$$\mathbf{J}_i = -D_i\rho_s\boldsymbol{\nabla}\zeta_i + \frac{D_i c_i \rho_s \Omega\gamma}{kT}\boldsymbol{\nabla}\kappa, \quad (4)$$

where the first term follows from Fick's law, and the second term gives the contribution from capillarity [3], where γ is the surface energy, $\boldsymbol{\nabla}$ denotes the gradient on the surface, $\kappa = \nabla^2 h$ is the curvature, Ω is the atomic volume, D_i is the diffusion constant of species i, and ρ_s is the areal density of mobile atoms, which could depend on the ion flux [4].

While the evolution of the perturbation in composition ζ is determined by the deviation of the ratio of the effective surface fluxes $\delta F_i + \boldsymbol{\nabla}\cdot\mathbf{J}_i$ of the A and B species from the stoichiometric ratio $c_b/(1 - c_b)$ in Eq. (1), mass conservation requires the growth of surface height to be proportional to the sum of the effective fluxes; the evolution equations for the perturbations can then be written as

$$\Delta\frac{\partial\zeta}{\partial t} = \Omega[(c_b - 1)(\delta F_A + \boldsymbol{\nabla}\cdot\mathbf{J}_A) + c_b(\delta F_B + \boldsymbol{\nabla}\cdot\mathbf{J}_B)],$$
$$\frac{\partial h}{\partial t} = -\Omega[\delta F_A + \delta F_B + \boldsymbol{\nabla}\cdot\mathbf{J}_A + \boldsymbol{\nabla}\cdot\mathbf{J}_B]. \quad (5)$$

Using the expression for surface composition in Eq. (2), Eqs. (3) and (4), and adopting the definitions

$$H = \frac{h}{\Delta}, \qquad L = \frac{\Omega\gamma}{kT},$$
$$B_A = \frac{D_A\rho_s\Omega^2\gamma}{kT}, \quad \text{and} \quad f_A = FY_A\Omega,$$

the evolution equations, to linear order in the perturbations, take the form

$$\frac{\partial\zeta}{\partial t} = A\nabla^4 H + B\nabla^2\zeta - C\zeta, \quad (6a)$$
$$\frac{\partial H}{\partial t} = -A'\nabla^4 H + B'\nabla^2\zeta + C'\zeta + D'\nu_h, \quad (6b)$$

where the coefficients of the terms on the right-hand side are given in Table I.

A key feature of Eq. (6) is the coupling between the height and composition modulations. To study the effect of this coupling on the evolution of sputter ripples, we look for solutions of the form $(H, \zeta) = (H_0, \zeta_0 e^{i\phi})\times e^{i(k_x x + k_y y + \omega t) + rt}$, where ϕ is the relative phase between the height and composition modulations, k_x and k_y are wave vectors, ω is the wave speed, and r gives the growth rate of the perturbations. Of particular interest is the fastest growing "mode" that will be observed for a given set of material parameters. Although an exact analytical solution for this mode is difficult, below we derive an approximate solution and show that it closely agrees with the numerical solution of Eq. (6). Since the coupling effects should be most significant in a 50–50 alloy, we will set $c_b = 0.5$ in all of the calculations.

In order to obtain an approximate solution, we first observe that the terms on the right-hand sides of the two equations in (5) are equal in magnitude. Therefore, $\Delta\partial\zeta/\partial t$ will be comparable to $\partial h/\partial t$ only if the surface composition changes by $\sim O(1)$ in the time it takes to change the surface height by an amount Δ. We can rule out this possibility, since removing a few layers of material from the slightly perturbed surface cannot lead to a significant variation in surface composition; this amounts to assuming that composition variations remain in steady state as the ripples grow in amplitude, or $\partial\zeta/\partial t \approx 0$ in Eq. (6a). Next, we consider the factors that lead to this steady state condition.

The growth in height perturbations induced by roughening mechanisms during sputtering [1] also induces the growth of composition modulations due to differences in the yields and diffusivities of the two species as shown by the first term (with coefficient A) on the right-hand side of Eq. (6a). The growth in composition is balanced by the next two terms: The term proportional to B comes from Fick's law, and the last term, *unique to sputtering*, accounts for the relaxation in composition brought about by the ion flux—any deviations from the surface composition c_s are compensated by increased sputtering of the species enriched by the modulation ζ. Compared to this "local" relaxation, surface diffusion requires transport of material on the scale of the wavelength λ of the modulations—we can show that it will be significant only when $\lambda < \lambda_c = 2\pi\sqrt{B/C}$. For typical values of material parameters (refer

TABLE I. Coefficients of the terms on the right-hand side of the evolution equations in Eq. (6). R_Y and R_D denote, respectively, the ratios Y_B/Y_A and D_B/D_A.

$A = B_A c_s(1 - c_b)(\frac{R_D}{R_Y} - 1)$	$A' = B_A c_s(1 + \frac{(1-c_b)}{c_b}\frac{R_D}{R_Y})$
$B = B_A(1 - c_b + c_b R_D)\frac{1}{L\Delta}$	$B' = B_A(1 - R_D)\frac{1}{L\Delta}$
$C = f_A(1 - c_b + c_b R_Y)\frac{1}{\Delta}$	$C' = f_A(R_Y - 1)\frac{1}{\Delta}$
	$D' = f_A\frac{R_Y}{(1-c_b)+R_Y c_b}\frac{1}{\Delta}$

to Table II), we get $\lambda_c \approx 15$ nm, which is smaller than the wavelengths (in the range 50–500 nm) observed in sputtering experiments. We will therefore ignore the terms proportional to B and B' in the approximate analytical solution of the evolution equations.

Using the above approximations, Eq. (6a) can be solved for a 50–50 alloy to obtain the dimensionless ratio of the composition and height variations:

$$\frac{\zeta_0}{H_0} = \frac{2B_A\Delta}{f_A}\frac{Y_AY_B}{(Y_A+Y_B)^2}\left(\frac{Y_A}{Y_B}\frac{D_B}{D_A}-1\right)(k_x^2+k_y^2)^2. \quad (7)$$

This result can then be used in Eq. (6b) to obtain the growth rate r for any given set of the wave vectors (k_x, k_y), from which the fastest growing mode can be determined. As in the BH [1] analysis, this mode is modulated in the x (y) direction if $G_x > G_y$ ($G_y > G_x$). Taking $G_x > G_y$ without loss of generality, the wave vector of the fastest growing traveling wave is found to be

$$k_{\max} = k_A\sqrt{\frac{1+\frac{Y_A}{Y_B}}{1+(\frac{Y_A}{Y_B})^2\frac{D_B}{D_A}}}, \quad \text{where} \quad k_A = \sqrt{\frac{G_xf_A}{2B_A}} \quad (8)$$

is the corresponding wave vector for the A species (i.e., when $c_b = 1$). Also, the angular velocity of this mode is found to be $\omega = v_n k_x$, where $v_n = D'\Delta$ (given in Table I) is the steady state velocity of the sputtered surface. Finally, Eq. (7) shows that the composition and height modulations are either in phase (peaks rich in A) or out of phase (valleys rich in A), depending on the sign of $D_BY_A - D_AY_B$. We can understand this by noting that the net flux of atoms of a given species leaving the peaks for the valleys of a sinusoidal profile is proportional to their diffusivity D_i and their *kinetic* surface concentration c_i [refer to Eq. (4)]. Since c_A is proportional to Y_B as shown in Eq. (2), the valleys (peaks) will be richer in A if $D_AY_B > D_BY_A$ ($D_AY_B < D_BY_A$).

Next, we turn to a numerical solution of the evolution equations and compare these results with the analytical analysis. In the numerical calculations, we have used the physical parameters for sputtering of Si(001) by 1 keV argon atoms at room temperature [5] given in Table II. Treating Si as the A species of the AB alloy, the results for $k_{\max}$, phase ϕ, and the magnitude of the composition modulations are given in Figs. 2–4 as a function of the ratios D_A/D_B and Y_A/Y_B. Large variations in diffusivities of the two components should generally be expected, since the differences in their activation barriers can be significantly larger than kT. Also, the yields of the two species can differ by 1–2 orders of magnitude [6]. We have therefore allowed these quantities to vary from 1/100 to 100.

TABLE II. Parameters for sputtering of Si(001) by 1 keV argon ions at room temperature from Ref. [5]. The parameter B_A is estimated from the BH theory [1] using $\lambda = 50$ nm, and L is obtained by taking $\Omega = 0.02$ nm^3 and $\gamma = 1$ J m^{-2}.

f_A	B_A	L	Δ	ν_0	G_x	G_y
0.2 nm s^{-1}	6 nm^4 s^{-1}	5 nm	0.5 nm	1	1 nm	0.3 nm

The bottom frame in Fig. 2 shows that the wave number $k_{\max}$ (for ripples modulated along the x axis) predicted by Eq. (8) agrees closely with the numerical results. The figure also confirms the intuitive reasoning that the observed wave number for the alloy ripples should straddle the wave number for the individual species, or $\min(k_A, k_B) \le k_{\max} \le \max(k_A, k_B)$, where $k_B = k_A\sqrt{Y_BD_A/D_AY_B}$. When $Y_A/Y_B \ll 1$, the surface is rich in A, and therefore $k_{\max}$ is close to k_A, while it is close to k_B when $Y_A/Y_B \gg 1$. The phase angles of the ripples obtained from the numerical calculations (given in Fig. 3) are also in excellent agreement with Eq. (7). The close agreement of the wave numbers and the phase angles justifies the approximations made in deriving the analytical results.

From a practical perspective, perhaps the most significant result of this work relates to the degree of modulation in composition that can be achieved under normal sputtering conditions. In Fig. 4, we have plotted $|\zeta_0|$ for modulations with amplitude $h_0 = 20$ nm, typically observed for ripples with $\lambda \sim 50$–100 nm. The figure shows that, for a given ratio of D_A/D_B, there is a particular value of the ratio

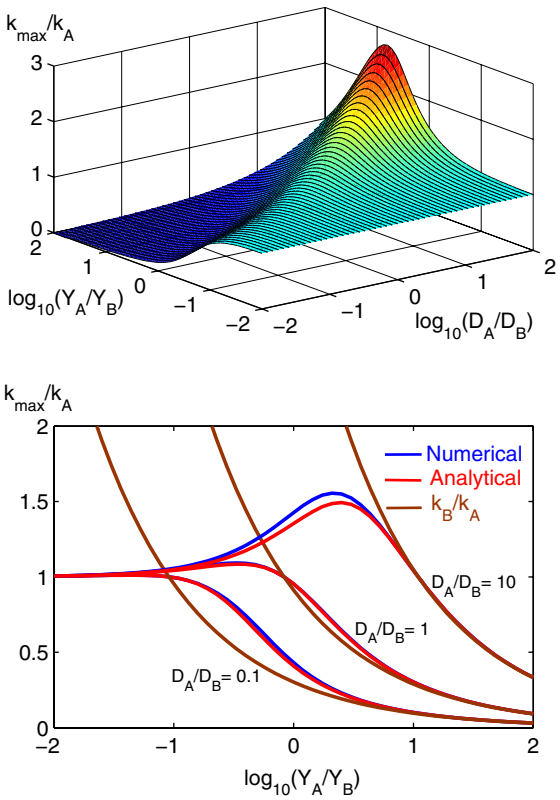

FIG. 2 (color online). (Top) Wave number of the fastest growing mode obtained from the numerical solution of Eq. (6) for material parameters in Table II. (Bottom) Comparison of the numerical and analytical results [from Eq. (8)] for $k_{\max}/k_A$. The brown curves correspond to k_B/k_A.

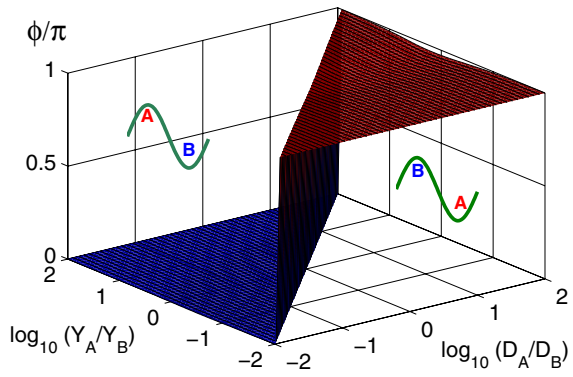

FIG. 3 (color online). Phase angle between the composition and height modulations, ϕ obtained from the numerical solution of Eq. (6) for material parameters in Table II. The peaks (valleys) are enriched with the A species when $\phi = 0$ ($\phi = \pi$).

Y_A/Y_B for which the composition modulation is the largest—for very large or very small values of Y_A/Y_B, the surface composition c_s is close to zero or one, and the formation of ripples cannot significantly alter this composition. On the other hand, intermediate values of Y_A/Y_B can allow for larger variations in surface composition. Indeed, the plot for $D_A/D_B = 33$ in Fig. 4 shows a maximum modulation of $\zeta_0 \approx 0.35$ at $Y_A/Y_B \approx 3$, which indicates that the peaks and valleys are highly enriched in A ($c = 0.85$) and B ($c = 0.15$), respectively. Also, the ratio $|\zeta_0|/H_0$ predicted by Eq. (7) is in good agreement with the numerical calculations. The composition modulations can be experimentally measured using spatially resolved scattering techniques (see, for example, Ref. [7]).

While a greater degree of alloy decomposition can be achieved by increasing D_A/D_B, for a given material system where this ratio is fixed, the degree of decomposition can be altered by varying the ion flux F. We find from Eq. (7) that $|\zeta_0|/H_0$ scales with $k_{\max}^4/F$—depending on the experimental conditions, we can identify two types of scaling laws for $k_{\max}$ due to the flux dependence of the areal density of mobile atoms ρ_s. In the low-flux and high-temperature limit, ρ_s should be independent of the ion flux as it is determined primarily by thermal adatom generation, whereas in the high-flux, low-temperature regime, $\rho_s \sim F$ [4]. Therefore, in the former case, Eq. (8) shows that $k_{\max} \sim \sqrt{F}$, while it is independent of the flux in the latter case. Subsequently, a linear scaling $\zeta_0/H_0 \sim k_{\max}^4/F \sim F$ is expected in the low-flux, high-temperature limit, and a scaling law $\zeta_0/H_0 \sim 1/F$ is obtained in the high-flux, low-temperature limit.

In summary, we have shown that sputter ripples on alloy surfaces will also be modulated in composition due to differences in the yields and diffusivities of the alloy components. For alloy sputtering, we have obtained analytical results for the fastest growing ripple wavelengths,

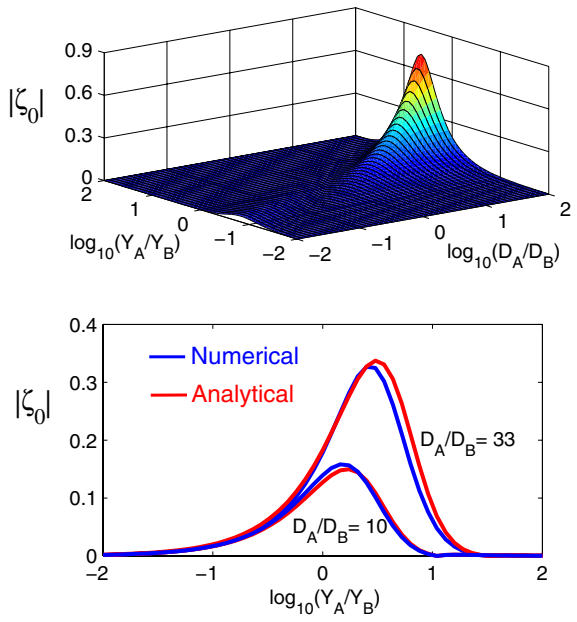

FIG. 4 (color online). (Top) Modulation in composition for ripples with an amplitude $h_0 = 20$ nm, obtained from the numerical solution of Eq. (6) for material parameters in Table II. (Bottom) Numerical and analytical results [from Eq. (7)] for $|\zeta_0|$ plotted for two different values of D_A/D_B.

the degree of kinetic alloy decomposition, and the conditions under which the ripple topography and composition modulations are in or out of phase. Our work shows that sputtering can be used as a tool to simultaneously achieve patterning of both the topography and the composition of alloy surfaces.

We hope that this work will motivate systematic experimental studies on sputter ripples in alloy systems. The research support of the NSF through Grant No. CMS-0210095 and the U.S. DOE under Contract No. DE-FG02-01ER45913 is gratefully acknowledged.

*Vivek_Shenoy@brown.edu

[1] R. M. Bradley and J. M. E. Harper, J. Vac. Sci. Technol. A **6**, 2390 (1988).
[2] For reviews, refer to U. Valbusa, C. Borangno, and F. R. de Mongeot, J. Phys. Condens. Matter **14**, 8153 (2002); M. A. Makeev, R. Cuerno, and A. L. Barabasi, Nucl. Instrum. Methods Phys. Res., Sect. B **197**, 185 (2002).
[3] W. W. Mullins, J. Appl. Phys. **28**, 333 (1957).
[4] W. L. Chan and E. Chason, Phys. Rev. B **72**, 165418 (2005).
[5] B. Ziberi *et al.*, Phys. Rev. B **72**, 235310 (2005); R. Gago *et al.*, Phys. Rev. B **73**, 155414 (2006).
[6] P. Sigmund, Nucl. Instrum. Methods Phys. Res., Sect. B **27**, 1 (1987).
[7] J. B. Hannon *et al.*, Phys. Rev. Lett. **96**, 246103 (2006).